REPORT DOCUMENTATION PAGE

Form Approved
OMB No. 0704-0188

PLEASE DO NOT RETURN YOUR FORM TO THE ABOVE ORGANIZATION.

1. REPORT DATE *(DD-MM-YYYY)*	2. REPORT TYPE	3. DATES COVERED *(From - To)*
15-01-2010	Conference Proceeding	

4. TITLE AND SUBTITLE
Ocean Data Assimilation Guidance Using Uncertainty Forecasts

5a. CONTRACT NUMBER

5b. GRANT NUMBER

5c. PROGRAM ELEMENT NUMBER
0602435N

6. AUTHOR(S)
Emanuel Coelho, Clark Rowley, Gregg Jacobs

5d. PROJECT NUMBER

5e. TASK NUMBER

5f. WORK UNIT NUMBER
73-6279-09-5

7. PERFORMING ORGANIZATION NAME(S) AND ADDRESS(ES)
Naval Research Laboratory
Oceanography Division
Stennis Space Center, MS 39529-5004

8. PERFORMING ORGANIZATION REPORT NUMBER
NRL/PP/7320-09-9339

9. SPONSORING/MONITORING AGENCY NAME(S) AND ADDRESS(ES)
Office of Naval Research
800 N. Quincy St.
Arlington, VA 22217-5660

10. SPONSOR/MONITOR'S ACRONYM(S)
ONR

11. SPONSOR/MONITOR'S REPORT NUMBER(S)

12. DISTRIBUTION/AVAILABILITY STATEMENT
Approved for public release, distribution is unlimited.

13. SUPPLEMENTARY NOTES

14. ABSTRACT

This paper discusses preliminary tests on using predicted forecast errors to estimate the impact of observations in correcting the Naval Research Laboratory (NRL) tide resolving, high resolution regional version of the Navy Coastal Ocean Model (RNCOM) assimilating local observations processed through the NRL Coupled Ocean Data Assimilation (NCODA) system. Since there will always be a shortfall of data to constraint all sources of uncertainty there is an obvious advantage to optimally guide observations to reduce model errors that could be producing the most negative impacts. The importance of this topic has been further heightened in oceanic applications by the advent of Underwater Automated Vehicles (UAVs) that can bring persistent observations but need to be told where to go and when, following regular schedules. This works tests a technique named the Ensemble Transform Kalman Filter (ETKF) that can be used to automate such adaptive sampling guidance and has been successfully applied for atmospheric modeling optimization. The ETKF uses an ensemble of state-fields from a certain initialization time and rapid low rank solutions of the Kalman filter equations to estimate integrated predicted error reduction for selected target ensemble variables, or combinations of variables, over areas and forecast ranges of interest. The error estimates are produced through independent RNCOM runs using perturbed forcing and initial conditions constrained at each analysis time by new estimates of the analysis errors as provided by NCODA, using a technique named Ensemble Transform (ET).

15. SUBJECT TERMS
UAVs, ensemble transform, assimilation, forecasting

16. SECURITY CLASSIFICATION OF:			17. LIMITATION OF ABSTRACT	18. NUMBER OF PAGES	19a. NAME OF RESPONSIBLE PERSON
a. REPORT	b. ABSTRACT	c. THIS PAGE			Clark D. Rowley
Unclassified	Unclassified	Unclassified	UL	8	19b. TELEPHONE NUMBER *(Include area code)* 228-688-5809

Ocean Data Assimilation Guidance Using Uncertainty Forecasts

E. F. Coelho
University of Southern Mississippi
Stennis Space Center, MS 39529 USA

C. Rowley and G. Jacobs
Naval Research Laboratory
Stennis Space Center, MS 39529 USA

Abstract- This paper discusses preliminary tests on using predicted forecast errors to estimate the impact of observations in correcting the Naval Research Laboratory (NRL) tide resolving, high resolution regional version of the Navy Coastal Ocean Model (RNCOM) assimilating local observations processed through the NRL Coupled Ocean Data Assimilation (NCODA) system. Since there will always be a shortfall of data to constraint all sources of uncertainty there is an obvious advantage to optimally guide observations to reduce model errors that could be producing the most negative impacts. The importance of this topic has been further heightened in oceanic applications by the advent of Underwater Automated Vehicles (UAVs) that can bring persistent observations but need to be told where to go and when, following regular schedules. This works tests a technique named the Ensemble Transform Kalman Filter (ETKF) that can be used to automate such adaptive sampling guidance and has been successfully applied for atmospheric modeling optimization. The ETKF uses an ensemble of state-fields from a certain initialization time and rapid low rank solutions of the Kalman filter equations to estimate integrated predicted error reduction for selected target ensemble variables, or combinations of variables, over areas and forecast ranges of interest. The error estimates are produced through independent RNCOM runs using perturbed forcing and initial conditions constrained at each analysis time by new estimates of the analysis errors as provided by NCODA, using a technique named Ensemble Transform (ET). The skills of these systems in tracking the RNCOM forecast errors and predicting the reduction in forecast error from a set o possible observations were tested using local profile measurements off the East Philippines. Results show areas of larger uncertainty close to the major spatial gradients as one could anticipate and a good accuracy of error estimates with an high spread-skill (i.e. ensemble estimates had the ability to correctly separate the small ensemble spread well correlated with the smaller observed errors from the larger ensemble spread well correlated with the larger observed errors). This consistency is a necessary condition to allow the ETKF to accurately predict the impact of the observations in reducing model errors. These ETKF skills were then tested by comparing the vertically averaged predicted temperature corrections based on the local measurements with the vertically averaged magnitude of the observed changes between two consecutive forecasts (before and after assimilating the data). Results showed the system had skills to accurately predict RNCOM errors and the impact of observation networks in reducing the error of model state-variables.

I. THE HIGH RESOLUTION NAVY COASTAL OCEAN MODEL

The relocatable Navy Coastal Ocean Model (RNCOM) is based on a standardized development and an efficient configuration management to facilitate transitions of new tools and real-time configurations of regional high resolution (order I km) ocean predictions [1]. The physics and numerical procedures of NCOM are based on the Princeton Ocean Model (POM) and a Sigma/Z-level Model (SZM). It solves a three-dimensional, primitive equation, baroclinic, hydrostatic and free surface system using a cartesian horizontal grid, a combination of σ/z level (i.e. bottom-following/constant depth) vertical grid and implicit treatment of the free surface. Horizontal eddy coefficients are calculated based on maximum grid-cell Reynolds number criteria, and vertical eddy coefficients are calculated using the Mellor-Yamada Level 2 turbulence closure scheme. For meso-scale real-time applications, boundary conditions are taken from an operational run of the global NCOM (GNCOM). The global model assimilates satellite altimetry and sea-surface temperature (SST) data using a combination of model analysis and data. Since the global NCOM does not include tides, these are explicitly inserted in the RNCOM nests through the boundary conditions and local forcing terms.

The data assimilation is performed using the Navy Coupled Ocean Data Assimilation (NCODA) system [2]. It is based on a three-dimensional multivariate optimum-interpolation (MVOI) data assimilation system, that will in the future apply variational methods (3DVAR and 4DVAR), cycling in real-time to provide new analysis and model updates of the ocean state variables (temperature, salinity, velocity and sea surface height). Additional capabilities built into the system, includ flow-dependent background-error correlations and background-error variances that vary in space and evolve from one analysis cycle to the next. It also includes a data quality-control system with multivariate analysis using feedback of forecast fields and prediction errors in the quality control of new observations.

Typical runs of these systems use 72 or 96 hours forecast ranges, horizontal grids of 3km resolution and 50 vertical levels, of which the upper 30 are sigma layers. The topography is usually taken from the Naval Research Laboratory global 2 minute resolution ocean bathymetry data base (NRL DBDB2). Atmospheric forcing usually consists of hourly fields of sea level air

0-933957-38-1 ©2009 MTS

pressure, wind stress, solar and long wave radiation, and 2m air temperature and humidity from 15-km resolution Coupled Ocean-Atmosphere Modular Prediction System (COAMPS) analysis/forecast runs and interpolated to the ocean model grids. Operational runs start daily 24 hours prior to analysis time from a snapshot of the previous run. The first 24 hours are used for the model initialization by sequentially adding the increments computed by NCODA (slow insertion of model corrections), such that at the analysis time (hour 0) the model fields reproduce the best analysis estimates as delivered by NCODA. Model outputs are then post-processed to standard levels and made available through netCDF files. These files can include a full or partial range of variables from the native model output.

The NCODA interpolation problem is formulated as:

$$x_a - x_b = P_b H^T (H P_b H^T + R)^{-1} [y - H(x_b)] \quad (1)$$

where $\mathbf{x_a}$ is the analysis vector, $\mathbf{x_b}$ is the time dependent background vector, $\mathbf{P_b}$ is a time dependent background error covariance matrix, $\mathbf{H}$ is the observational functional operator, $\mathbf{R}$ is the observation error covariance matrix, and y is the observation vector at a specific update cycle. The forward model $\mathbf{H}$ converts forecast model variable to an observed variable and, as used here, is a spatial interpolation of the forecast model grid to the observation location performed in three dimensions. Therefore, $\mathbf{HP_bH^T}$ is the background-error covariance between observation locations, and $\mathbf{P_bH^T}$ the error covariance between observation and grid locations. The quantity $\{y - \mathbf{H(x_b)}\}$ is referred to as the innovation vector and $\mathbf{x_a} - \mathbf{x_b}$ is the increment (or correction) vector. Observations are assimilated close to their measurement times within the update-cycle time window by comparison against time-dependent background fields using the first-guess at appropriate time (FGAT) method. The ocean variables are analyzed simultaneously in three dimensions such that the observation vector contains all of the synoptic temperature, salinity and velocity observations that are within the geographic and time domains of the forecast model grid and update cycle. The velocity increments are forced to be in geostrophic balance with the geopotential increments which, in turn, are in hydrostatic balance with the temperature and salinity increments. Prior to an analysis the innovation vector is normalized by the background error at the observation locations, and after an analysis the increment vector is scaled by the background error at the grid locations.

Typical implementations of NCODA use more than 30 vertical levels, with the background error variances being computed from the increments using a recursive filter model with a time constant of 10 days and imposing geostrophic cross-correlations on the velocity errors computed from the mass variables. The first baroclinic Rossby radius of deformation is usually selected as the local spatial correlation length scale for horizontal interpolations between observations and observations and grid locations. The vertical correlation length scale are computed from local background density vertical gradients. The system uses a First Guess at Appropriate Time (FGAT) window of 24 hours, usually set as 12 hours around analysis time. When no data is available for long periods of time, error variances are relaxed towards climate variability. The NCODA system also includes a complete quality control system that assesses the error probability of each individual observation and the final profile. These profile data are then processed with the model runs to produce data match-up files that are used to run diagnostics of the model forecast errors and ensemble performances.

For this experiment the RNCOM was run on the domain 15N 113E, 18.3N 121E (see Fig. 1), from 1 March to 4 April 2009. The boundary conditions were taken from the Global run of NCOM and atmospheric forcing from the regional 15km COAMPS [3] run by the Fleet Numerical Meteorological and Oceanographic Center (FNMOC). Tides were introduced at the boundaries and through local tidal potentials. The horizontal grid spacing was set at 3km and used 50 sigma/z levels in the vertical. Observations from global data bases were assimilated over the full period, including satellite altimetry and SST. From 17 March to the end of the simulation period there was also one glider in the area providing regular profiles and ship observations during the period 21-23 March.

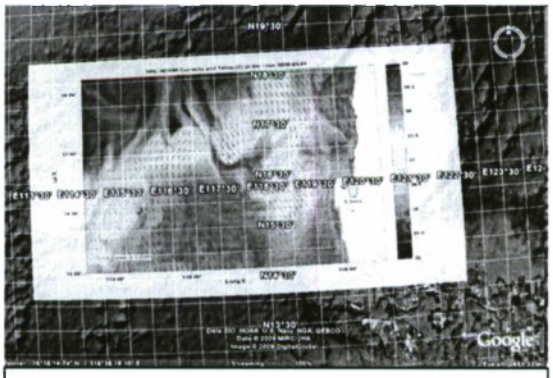

Fig. 1 – Model domain run March-April 2009

Local dynamics where characterized by the evolution of a cold core gyre in the middle-northern portion of the domain, typical in the region for this time of the year, intruding westward in depth towards the coast. Further south, the temperature fields where more homogeneous and stable throughout the simulations period. Overall in the area there was a sharp well defined upper layer, with a steep thermocline ranging between 50 to 100m depth. The tides in the area were small but still capable of some perturbations of the thermocline within the tidal cycles, suggesting a propagation of mild internal tide interfacial modes in the region.

The system responded significantly to the assimilation of local observations as shown in Fig.2. The upper bar plot in this figure shows water temperature mean errors (bias) for 19-23 March averaged through out the domain in the upper 400m. The middle plot shows the value of the maximum temperature bias error observed in the upper 400m and the lower plot shows the average of the profile RMS errors. The larger errors were observed at the thermocline levels (50-100m depths) and became smaller after 21 March after the assimilation of the ship observations. In these bar plots the green bars correspond to the comparisons between observations and 24-48 hour forecasts (prior to assimilating the test data) and use the same observations as the blue bars that compare the data with the consecutive run of the model using the 0-24 hours forecasts after assimilating the independent test data. By comparing these two bars we can get a proxy of the impact of the observations that were assimilated between the two consecutive runs.

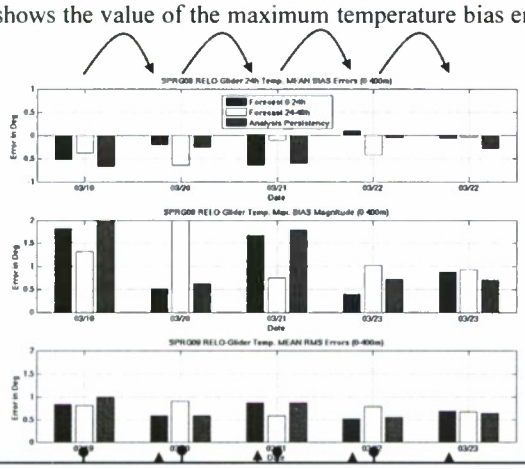

Fig. 2 - Comparisons of upper 400m mean temperature forecast errors before assimilating test data (48 hours forecasts – green bars) with the errors after assimilating test data (24 hours forecasts – blue bars).

If we define $\Delta = e_{i\ (\text{BEFORE ASS.})} - e_{i+1\ (\text{AFTER ASS.})}$, where e_i corresponds to the forecast mismatch RMS before the assimilation of test data and e_{i+1} to the forecast mismatch after the assimilation of the data (corresponding to the green and blue bars displayed in the lower plot of Fig.2), we can expect the daily mean Δ to be positive during the period shown in the picture (i.e. observations had a positive impact in reducing forecast errors). The overall mean Δ was positive (with a 0.04°C average) and had an RMS of 0.15°C. This shows the system had a small but positive response to the assimilation of local observations that should be reproduced by the ensemble based error models (e.g. [4], [5]), as it will be expanded in the next sections.

II. ERROR MODELING USING THE ENSEMBLE TRANSFORM

The errors in the RNCOM variable forecasts are determined by multiple sources of uncertainty as detailed in [4]. They are associated with the model initialization and boundary conditions, numerical approximations, modeling strategies, impact of under-sampling in the assimilation process and unresolved scales. To address the initialization error this work uses the ensemble transform (ET) method to produce perturbations at each analysis time following the approach detailed in [5] and [6]. The ET uses the best available estimate of analysis error covariance to transform forecast perturbations into analysis perturbations by finding K distinct linear combinations of K forecast perturbations. For operational implementations, the NCODA analysis error variance is used to renormalize each new ET ensemble. The ET analysis perturbations are then added to the best available analysis (in this case produced by the RNCOM-NCODA) to create K initial states. These K initial states are then integrated forward in time using the non-linear model to create the next ensemble forecast that will be the starting point for the ET transformation that will generate the initial conditions for the subsequent ensemble forecast once the subsequent analysis is available. As such, the ET ensemble generation scheme is a cycling scheme with strong similarities to a breeding scheme. This technique does not account for additional error sources that could develop during the forecast period through the boundaries and/or through unrepresented numerical errors and approximations.

The RNCOM ensembles also represent the errors due to uncertain atmospheric forcing by using an ensemble of atmospheric perturbations and allow each ocean run to have an independent atmospheric forcing, therefore augmenting the domain spanned by the the ensemble of initial states. This is done using atmospheric forcing perturbations as detailed in [7], based on spatially-varying time shifts of the atmospheric forecast, with a choice of parameters to provide a well developed spread of atmospheric perturbations. This method is mostly adequate when predicted atmospheric fields contain the forecast features of interest, but they are misplaced in space and time.

The ensembles resulting from combining the ET and the perturbed atmospheric forcing are then used to predict how uncertainties of the ocean fields will evolve in space and time. Typical implementations of ensembles use 40 independent members perturbed from a control run that performs the full data assimilation cycle, where each one of the simulations uses independent atmospheric forcing and perturbed initial conditions as detailed above.

For this experiment off the East Philippines, the system was implemented using 32 ensemble members centered around a control run assimilating the local data. The ensemble spread of these runs was reset at each running cycle using the NCODA analysis error variances. Fig. 3 shows an example of the temperature fields at 50m depth. The map on the left corresponds to the temperature estimates at 00:00 of 23 March and the map on the right shows the corresponding ensemble spread (i.e. the standard

deviation of the ensemble member temperatures around the ensemble mean). Note regions of larger predicted errors concur with the areas of larger gradients and time variability. The layer of 50m corresponds roughly to the upper level of the thermocline and was the most dynamic and uncertain through out the experiment. Since we have an ensemble population larger than 30, using the central limit theorem one can assume there will be a normally distributed envelope variable that can be estimated by the ensemble (i.e. the ensemble members are normally distributed). Based on the ensemble spread as shown in the figure for a normal distribution and using the number of samples equal to 32, we expect the ensemble mean temperatures errors to be smaller than 0.7°Cg up to 95% when the ensemble spread is 2°C and 0.3°C when the ensemble spread is 1°C. This analysis can provide an immediate application of the ensemble as a proxy error estimate. Fig. 4 shows how the predicted ensemble spread compared with the magnitudes of the 0-24 hour forecast mismatches ($|e_i|$). The upper scatter plots show the temperature and salinity ensemble spread vs the observed $|e_i|$ for days 17 March (before the ship data being assimilated) and for 23 March (during ship observations). The maps below each scatter diagram show the mean ensemble spread at the analysis time and the white crosses show the locations were data was available and used to compute the model mismatches e_i.

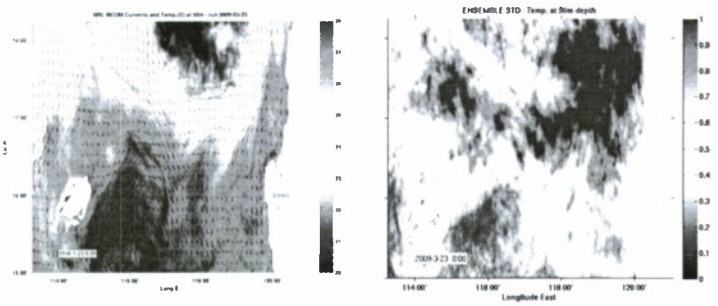

Fig. 3 – RNCOM and Ensemble estimates of water temperature at 50m depth for 00:00 March, 23 2009

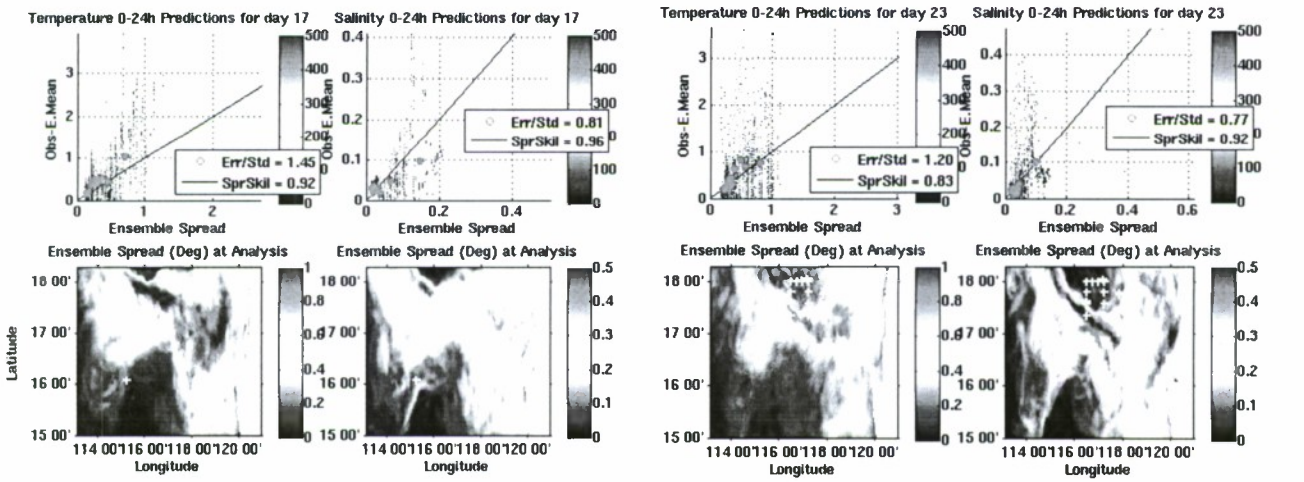

Fig. 4 - The upper scatter plots show the TEMPERATURE and SALINITY ensemble spread vs the observed forecast errors (e) for days March 17 on the left (before the ship data being assimilated) and for March 23 on the right (last day of ship observations). The maps below each scatter diagram show the mean ensemble spread at the analysis time and the white crosses show the locations were data was available and used to compute the model mismatches. The color of each individual estimate displayed as the small dots corresponds to the depth of the observation, accordingly to the color code displayed in the bars on the right (in meters).

Since ensemble variance is designed to be a predictor of the true variance it is not comparable to single measurements of squared model-data mismatches. To account for this the observed squared model mismatches were used to estimate observed error variances by ordering the data pairs from smallest ensemble variance to largest ensemble variance and then grouping the data pairs into 10 approximately equally populated bins. Within each bin, the bin averaged squared model-data mismatches were computed together with the bin-averaged ensemble variance. Since both of these quantities are sample variances, they are comparable. In order to keep the state-variable units this binning and averaging was done using the magnitudes of the forecast mismatches and the ensemble standard deviation rather than the variances. These quantities are displayed in Fig.4 as the large red dots in the scatter diagrams. For the ensemble to be accurate, these large red dots should be aligned along a positive slope and ideally along the main diagonal, highlighted as a black line on the plots. The skill is represented by the metric "SprSkil" corresponding to the bin correlation changing between 0 and 1. A value of SprSkil=1 represents a perfect spread-skill relation and values above 0.5 can be considered good ensemble spread-skill (i.e. the ensembles have the ability to correctly separate the small

ensemble spread values correlated with the smaller observed errors, from the larger ensemble spread values correlated with the larger observed forecast errors). Another relevant metric is the mean ratio between measured magnitudes of model-data mismatches and ensemble spread, (Err/Std in the plots), which represents the ensemble skill in terms of correctly predicting the magnitudes of the errors. Values higher than 1 indicate that the ensemble is under-dispersive (under-predicts the error magnitude and error bins are above the diagonal line) and values below 1 indicate that the ensemble is over-dispersive (over predicts forecast error magnitudes such that error bins are below the main diagonal). We can see that for temperature the ensemble was over-dispersive and under-dispersive for salinity.

The assimilation of ship observations in days 21-22 March appears to have reduced the ensemble spread in temperature (smaller predicted errors) and the ratio Err/Std became closer to 1. For salinity the ensemble spread increased along the sharp fronts and became slightly more under-dispersive. The larger differences between the ensemble estimates and the observed model-data mismatches were seen between the 50m and 150m isobaths, near the mixed layer depth.

III. Targeting Observations to Reduce Uncertainties

The problem of identifying the best location for deploying mobile observation platforms is often called the adaptive sampling or targeting observation problem. The importance of this topic has been heightened in oceanic applications by the advent of Autonomous Underwater Vehicles (AUVs). Planning the missions of these platforms includes updating reference way-points on regular schedules such that one must solve the adaptive sampling problem before some critical decision time. This work uses the Ensemble Transform Kalman Filter (ETKF) technique proposed by [8] and applied by [9] to adaptive sampling in atmospheric modeling applications. The ETKF uses the error estimates produced by the ensemble forecast as detailed in the previous section, and rapid low rank solutions of the Kalman filter equations to solve the targeting observation problem. The first step of the method is to identify the areas of interest inside the simulation domain here named as the **target box** and a forecast time called a **verification or target time** at which one wishes the adaptive supplemental observations taken at an earlier **observation time** to produce a maximum effect defined by a cost function. For the present example the cost functions to be minimized were the ensemble forecast variance (taken as a proxy of the forecast error magnitude) for ocean temperature profiles.

This technique assumes the analysis error covariance at the observation time can be estimated by $\mathbf{P}^{r}_{e} = \frac{\mathbf{X}^{r}\mathbf{X}^{rT}}{K-1}$ where $\mathbf{X}^{f}$(NxK) is the matrix with the ensemble N state-variables forecasts at the observation time and K is the number of ensemble members. However, these perturbations should be consistent with the best available guess of the error variance of an analysis made using all of the observations apart from the observations that will be targeted. To account for this constraint and as described in [9] a Transformation matrix $\mathbf{T}^{r}$ is applied so that, $\mathbf{X}^{r}=\mathbf{X}^{f}\mathbf{T}^{r}$. The transformation matrix $\mathbf{T}^{r}$ is computed using the ET technique and a guess of the analysis error covariance associated with the routine observations based on the ensemble predicted errors at those locations. The transformed perturbations $\mathbf{X}^{r}$ are then used produce a new error covariance $\mathbf{P}^{e}_{g}$. For this present study this transformation matrix was taken as an identity matrix, hence considering only the impact of observation platforms under the assumption that there were no routine data. The posterior analysis error covariance $\mathbf{P}^{f}_{etkf}$ after assimilating the ith feasible deployment of adaptive observations $\mathbf{y}^{a}_{i}$ will then be given by:

$$\mathbf{P}^{f}_{etkf} = \mathbf{P}^{e}_{g} - \frac{\mathbf{P}^{e}_{g}\mathbf{H}^{T}_{q}}{[\mathbf{H}_{q}\mathbf{P}^{e}_{g}\mathbf{H}^{T}_{q} - \mathbf{R}_{q}]}\mathbf{H}_{q}\mathbf{P}^{e}_{g} \qquad (2)$$

where H_q describes the mapping from the model state vector to the observation vector normalized by the inverse square root of the observation error covariance $\mathbf{R}^{-1/2}_{i}$ associated with the ith feasible deployment.

Using this result, we can now estimate $\mathbf{P}^{a}_{i} = \frac{\mathbf{X}^{a}_{i}\mathbf{X}^{aT}_{i}}{K-1}$ where $\mathbf{X}^{a}_{i}$ is the ensemble state matrix after including the targeted observations. The columns of $\mathbf{X}^{a}_{i}$ can be interpreted as transformed ensemble perturbations such that their covariance gives the analysis error covariance at the observation time assuming that the ith deployment of targeted observations had been assimilated i.e.: $\mathbf{X}^{a}_{i} = \mathbf{X}^{r}.\mathbf{T}_{ETKF}$, where T_{ETKF} is now determined by the eigenvectors and eigenvalues of the projections of the magnitude of the analysis perturbations, corresponding to the possible observations strategies, into $\tilde{\mathbf{H}}^{a}_{i}$. As shown in [8], this transform will not change along the forecast cycle; therefore the same transform matrix can be applied to the forecast perturbations to estimate the error covariance at the verification time $\mathbf{P}^{v}_{i}$. These results are hereafter used to infer the impact of observations taken at a given observations time on the error variance (computed as the standard deviation of $\mathbf{X}^{a}_{i}$) of the selected variables at a later time and at specific target locations $\mathbf{H}^{v}_{t}$. Therefore, the $\mathbf{RMS}(\mathbf{H}^{v}_{t}X^{f} - \mathbf{H}^{v}_{t}X^{a}_{i})$ should be a consistent estimator of the $\mathbf{RMS}(\Delta_{observed})$.

To find which of all feasible deployments of targeted observations has a larger impact in minimizing the selected cost function (e.g. the ensemble spread of selected variables), one can estimate the reduction in ensemble spread for each feasible grid point of the ensemble domain, taken as a single profile measurement, through a range of selected depths (for the present example 0 to 1000m to simulate a glider profile observation) and display the resulting information in the so-named summary maps as shown

here in Fig.5. Either by inspection or using automated tools to follow the areas of higher gains in both time and space (e.g. [9] and [10]), one can choose from the possible deployments those that will produce the most desired effect. To test these maps, target locations were selected along the subsequent day observation sites (red dots in the map) such that we can compare the changes in ensemble spread to the changes in model data mismatches. The summary map displayed in Figure 5 refers to the 23 March run, summarizing the suggested observation guidance from 00:00 24 March to 00:00 25 March, in reducing the mean temperature profile error over the target box at a forecast range of 48 hours after the analysis (i.e. 00:00 25 March). As anticipated, the area of higher impact in reduction of temperature error overlaps with the larger ensemble spread and fronts as displayed in Fig.3, that were closer to the target points, suggesting that an accurate characterization of the frontal system would be the one to reduce most the errors at the testing locations. The white dots show where observations actually took place during the observations window 00:00 24 March 24 to 00:00 25 March.

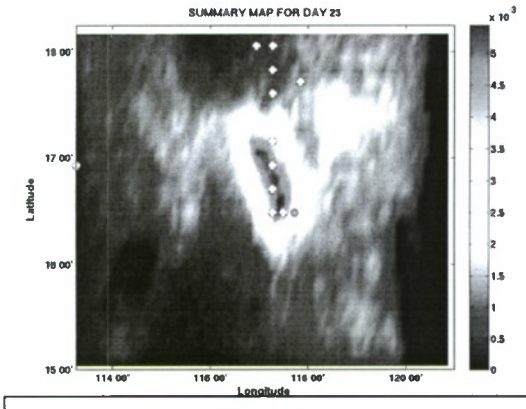

Fig. 5 - Summary Maps for T profile error reduction showing the relative impact of T-S independent observations during the window tau=0-24 in reducing the T errors at the sites highlighted as red dots, corresponding to where observations were made during tau=24-48. The white crosses show the places where observations were actually made and assimilated into the next run during the window tau=12-36

To positively validate the summary maps we require that the absolute value of the ETKF estimates of the model corrections over the target locations, after assimilating the available observations, be consistent with the actual forecast error reduction. One way to demonstrate this property is to take the actual measured model innovations and use the ETKF to predict their impact at the target or verification time, and then use other independent data to verify that the model forecast error variances were reduced accordingly, as discussed below. For this property to happen it will be necessary that the absolute value of the differences between the control runs at the verification time, before and after assimilating the observations to be consistent (i.e. well correlated) with the ETKF estimates at the target time for model corrections, through the available observations, up to the dynamic evolution of the ocean-state due to any possible changes in the atmospheric forcing and boundary condition. If they are well correlated then one can expect the suggestions provided by the summary maps should be also accurate, since the ETKF is consistently predicting the changes in forecast error. For this purpose Fig. 6 shows the changes in the forecast fields before and after the assimilation of the data that compare well with the error corrections the ETKF predicted based solely on the positions where observations took place, for 23 March. The map on the left shows the difference between the 48hours forecast of the run from 23 March with the 00:00 snapshot of the run from 25 March. The main cause for differences between these two snapshot (allowing for possible updates in the atmospheric forcing and some small changes in the boundary conditions) was the assimilation of the data from the locations highlighted as the white dots. The vertically averaged predicted temperature corrections (the map on the right) show patterns comparable to the vertically averaged magnitude of the observed changes between the two consecutive forecasts (before and after assimilating the data). Areas where the ETKF analysis predicts larger corrections are concurrent with the dynamic features associated with the frontal systems one would expect to be dynamically correlated with the observation sites. On the other hand, the observed corrections were more localized, as one could expect from the MVOI based on pre-set correlation length scales. The small area with large observed corrections close to the north boundary and close to 16N 114E seems to have been missed by the ETKF, due either to data other than profile assimilation, or to a small ensemble spread prediction at the observations time. The good qualitative agreement between these two maps suggests the ETKF was correctly predicting the impact of the corrections computed by the NCODA system and inserted into the RNCOM runs. One should note that this agreement exists in spite of the fact that the ETKF was applied prior to the actual observation time, used a fraction of the

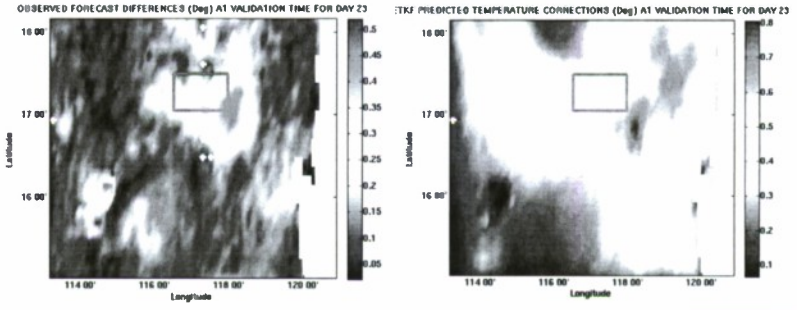

Fig. 6 - Vertically averaged predicted temperature corrections map (on the right) and the equivalent vertically averaged magnitude of the observed changes between two consecutive forecasts, before and after assimilating the data (map on the left).

ensemble spread as an estimate of the local observed innovation and ensemble-based covariances to estimate the overall corrections. The NCODA system uses a different method to compute the correction based on the measured differences between the observations and the control run at the observation location and the nearest time, and a multi-variate optimal interpolation method (e.g. [2]), with pre-defined correlation length scales (~50km in the present case). Between the two runs for 23 and 25 March, different atmospheric perturbations and boundary conditions were another source contributing to the observed change in the control runs that were not considered by the ETKF. This limitation might be overcome in future systems using fully coupled model dynamics and coupled data assimilation, such that ocean observations would reduce the uncertainty of the surface forcing and, in principle, account for the uncertainty in surface forcing in a rigorous way.

A more quantitative comparison between the ETKF predictions and observations of Δ can be found in Fig.7 as mentioned above. The mean magnitudes of the changes in model forecast mismatches are shown as the average values of the large red dot

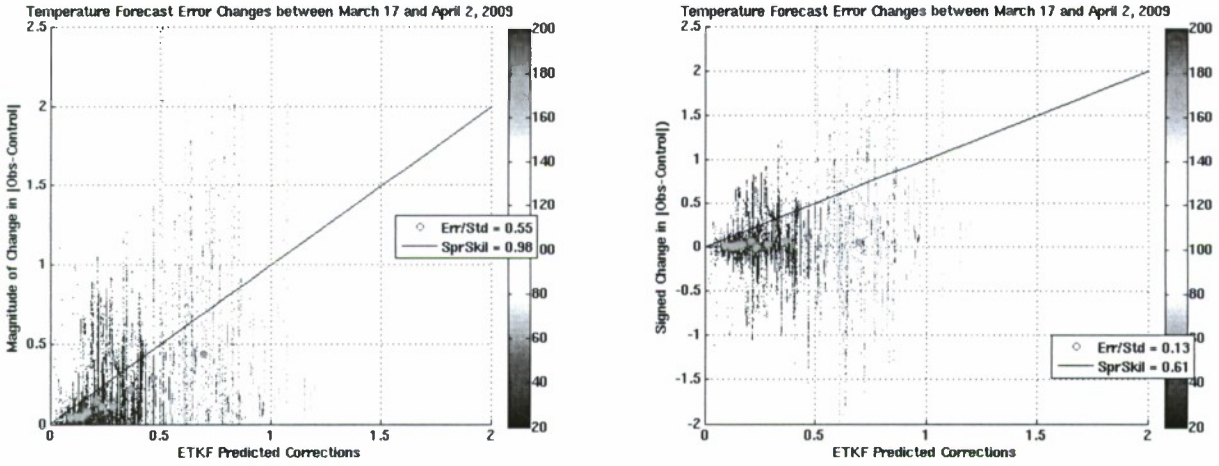

Figure 7 - Seatter diagrams showing the observed model mismateh ehanges before and after assimilating data ("Δ") vs. the square root of the ETKF predicted changes in model error variance. Colors eorrespond to the depth in meter were comparisons were made aceording to the eolorbar in the right. The diagram in the left shows the magnitude of "Δ" and the plot on the right show the signed "Δ" such that positive values correspond to decreasing model-data mismatches and negative values to increasing mismatches between two conseeutive runs and relative to the same test observations.

pixels of the left plot (note that the same binning is here required to compare ensemble variances with local observed model mismatches as explained above for Fig.4). This corresponds to a necessary condition for forecast error reduction and is the quantity that is directly estimated by the ETKF and used for adaptive sampling guidance. I.e. the ETKF will look for the observations that will produce larger changes in model error variance. The good overall correlation between this observed quantity and the ETKF predictions (see details below) measured by the parameter SprSkil = 0.98 and the good mean ratio between the observed vs predicted values (Err/Std = 0.58), shows the ETKF was accurately tracking these changes in model error variance. However, this is not a sufficient condition for model error reduction. Model error reduction will occur only when observations are taken at the right places and at the right times and is independent of the ETKF being able to correctly track model error variance. The actual forecast error reduction/increase can be estimated by the average of the pixels of the plot on the right (signed Δ), showing the mean change in model forecast error between consecutive forecasts such that if positive the errors were getting smaller and if negative the errors were getting larger. As the observations become more efficient in reducing the errors for the next run these two plots should converge. This feature can be well seen by using smaller sub-sets of observations, selected from the sites estimated to produce the larger impacts in error reduction. The plot in the right shows a poorer correlation (SprSkil = 0.61) and a mean ratio of Err/Std = 0.13, and suggests the observations during the period 17 March to 2 April were not enough to persistently produce an overall noticeable impact in reducing the model forecast errors as discussed in section 1. The average value for the RMS(Δ) was 0.15°C and MEAN(Δ) was +0.04°C. The corresponding mean square root of the model error variance change as predicted by the ETKF was 0.28Deg. This suggests the ETKF was over predicting the magnitude of the actual changes in error variance and that only roughly 30% of the actual changes in error variance were actually producing a forecast error reduction.

In order to see how these changes occur and if the ETKF was accurately separating the larger error variance changes from the smaller error variance changes one can note that the large red dots from both plots diagrams were correlated with the predicted error variances. Ideally these large red dots should be aligned along the diagonal line, but if aligned along a positive slope line

they will already show the ETKF was able to distinguish the large error changes from the smaller error changes and consequently was able to provide accurate adaptive sampling guidance. These slopes are estimated by the bin correlations and show the Spread-Skill relation (SprSkil in the plots). This parameter is positive for both plots showing that the ETKF had good skill in separating the errors and that there was on average a positive correlation between the error reductions at the observation sites with the error reduction at the validation sites, where the model mismatches were computed, confirming the guidance provided by the ETKF to be accurate.

IV. Final Remarks

During the spring 2009 a high-resolution NCOM (RNCOM) system was used to produce mean and error fields of meso-scale ocean states, northeast of the Philippines. These fields were used to test novel techniques to guide observation assets in reducing predicted model errors. The dynamics of the area included a sharp frontal system in the north, intruding colder water southward and a mild stable regime in the southern portion of the simulation domain. Atmospheric forcing was stable throughout the test period and a mild tidal regime was observed and predicted in the area. After a spin-up period, the daily mean residual prediction errors in temperature profiles were typically below 0.75°C, with larger values in the upper and lower limits of the thermocline (~50-100m depth), where stratification was stronger.

An ensemble of RNCOM runs was used to predict the dynamics of the forecast errors of the control simulations. These ensemble runs used perturbed initial conditions and perturbed atmospheric forcing as the main sources of uncertainty. At each analysis cycle, the initial condition perturbations were re-balanced using the ET technique that guarantees the ensemble error covariance at each analysis time to match closely the best estimate of the analyses error variance, as provided by the NCODA system after the objective analysis of the available observations. The forecast error predicted from the ensemble runs proved to be consistent with the observed forecast errors provided up to the data representation error, with a good spread-skill relation displaying a bin correlation always above 0.85.

The error forecasts produced by the ensemble system were then used to produce maps summarizing the predicted impact of each grid point taken as a possible observation site in reducing the errors of temperature profiles over selected sites. The predicted relative impact of the available observations assimilated into the model runs agreed well with the observed dynamics in the area and on average with model-data mismatches changes.

Overall, the work presented above showed that some level of predictability of stochastic environmental variables through numerical modeling can be achieved by Monte-Carlo methods, producing ensemble-based forecast error estimates along with the predicted state variables, using a limited number of ensemble runs. The focus of this effort was to use these estimates in target observation problem and to demonstrate the feasibility and anticipated accuracy of the ETKF system within the operational systems. It is anticipated that more validation tests will be required to complement this work using other independent data sets for validation, larger ensemble populations and different regions and dynamics. These extended analyses will allow further testing of the summary maps for operationally relevant variables and scenarios.

Acknowledgment

The authors thank Frank Bub, Mark Cobb, and Bruce Lunde from the Naval Oceanographic Office for their valuable contributions to this work.

References

[1] C. Rowley, P. J. Martin, and James A. Cummings, "The Naval Research Laboratory Relocatable Ocean Nowcast/Forecast System", ONR Journal of Underwater Acoustics, accepted, 2009.

[2] J. Cummings, "Operational multivariate ocean data assimilation". Q. J. R. Meteorol. Soc., 131, pp. 3583–3604, 2005.

[3] R.M. Hodur, "The Naval research laboratory's Coupled Ocean/Atmosphere Mesoscale prediction System (COAMPS)". Mon. Wea. Rev., 135, 1414-30, 1997.

[4] E.F. Coelho, G. Peggion, C. Rowley, G. Jacobs, R. Allard, and E. Rodriguez, "A Note on NCOM Temperature Error Calibration Using The Ensemble Transform", Joumal Marine Systems, doi:10.1016/j.jmarsys.2009.01.028, 2009.

[5] E.F. Coelho, J.-P. Fabre, C. Rowley, G. Jacobs, C. Bishop, J. Cummings and X. Hong, "Targeting Observations To Reduce Acoustic Prediction Uncertainty", ONR Joumal of Underwater Acoustics, in review, 2009.

[6] J.G. McLay, C.H. Bishop, and C.A. Reynolds, "Evaluation of the Ensemble Transform Analysis Perturbation Scheme at NRL". Mon. Wea. Rev., 136, 1093–1108, 2008.

[7] X. Hong, and C.H. Bishop,"Ensemble and Probabilistic Forecasting". In Proceedings IUGG XXIV General Assembly 2007, Perugia, Italy, 2-13 July, 2007.

[8] C.H. Bishop, B.J., Etherton and S.J. Majumdar, "Adaptive Sampling with the Ensemble Transform Kalman Filter. Part I: Theoretical Aspects". Mon. Wea. Rev. 129, 420-436, 2001.

[9] S.J. Majumdar, C.H. Bishop, B.J. Etherton and Z.Toth, "Adaptive Sampling with the Ensemble Transform Kalman Filter. Part II: Field Program Implementation". Mon. Wea. Rev., 130, 1356-1369, 2002.

[10] K. Haney, G. Gawarkiewicz, T.F. Duda, and P. Lermusiaux, "Nonlinear Optimization of Autonomous Undersea Vehicle Sampling Strategies for Oceanographic Data-Assimilation", in Joumal of Field Robotics 24(6), 437–448, 2007.